A Control Strategy for Upper Limb Robotic Rehabilitation With a Dual Robot System

Peter R. Culmer, Andrew E. Jackson, Sophie Makower, Robert Richardson, J. Alastair Cozens, Martin C. Levesley, and Bipin B. Bhakta

***Abstract*—This paper describes the development and use of the cooperative control scheme used by the intelligent pneumatic arm movement (iPAM) system to deliver safe, therapeutic treatment of the upper limb during voluntary reaching exercises. A set of clinical and engineering requirements for the control scheme are identified and detailed, which entail controlled, coordinated movement of a dual robot system with respect to the human upper limb. This is achieved by using a 6-DOF model of the upper limb that forms the controller's coordinate system. An admittance control scheme is developed by using this coordinate system such that robotic assistance can be varied as appropriate. Key controller components are derived, including kinematic and force transformations between the upper limb model and the dual robot task space. The controller is tested using a computational simulation and with a stroke subject in the iPAM system. The results demonstrate that the control scheme can reliably coordinate the dual robots to assist upper limb movements. A discussion considers the ramifications of using the system in practice, including the effects of measurement errors and controller limitations. In conclusion, the iPAM system has been shown to be effective at delivering variable levels of assistance to the upper limb joints during therapeutic movements in a clinically appropriate manner.**

***Index Terms*—Control system human factors, control systems, man–machine systems, rehabilitation robotics, robots.**

I. Introduction

STROKE is a major cause of adult disability. Approximately, 110 000 people have a stroke in England every year, and the estimated U.K. cost is £7 billion annually [1]. Impairment of the upper limb affects approximately 77% of the stroke population [2]. This is important because the upper limbs play a major role in everyday activities, and many tasks require the cooperative use of both hands.

The mainstay of upper limb rehabilitation after stroke is active exercise, with hands-on support from physiotherapists and occupational therapists. However, conventional rehabilitation services such as physiotherapy are severely resource-limited; therefore, patients often receive inadequate levels of therapeutic exercise [3]. Rehabilitation robotics has the potential to augment and improve existing modes of therapy, consequently easing the burden on health services. Several upper limb robotic systems have been developed, with evidence of positive effects on recovery [4]. For example, the Massachusetts Institute of Technology (MIT) Manus system is a planar device that connects to the forearm [5]. The GENTLE/s system interfaces to the forearm, providing three active DOFs with a passive upper arm support [6]. These and other distal attachment systems have drawbacks because the shoulder is not *actively* supported. This could potentially cause injury, e.g., by causing traction at the shoulder, and prevents the system from coordinating upper limb joints during assisted exercise.

More recent developments include exoskeleton systems such as ARMin II [7], which has six active DOFs: three at the shoulder, one for elbow flexion/extension, one for forearm prosupination, and one for wrist flexion/extension. Exoskeletons are mechanically more complex than distal attachment systems because they emulate the kinematic structure of the upper limb and must actuate the DOFs [8], [9]. This provides better support for the upper limb, but the complexity of the system is likely to make them expensive. A contrasting approach is taken by the REHAROB system [10] that uses two independent 6-DOF industrial robots to manipulate the upper limb. For a comprehensive review of upper limb rehabilitation systems, see [11].

An intelligent pneumatic arm movement (iPAM) system has been developed at the University of Leeds to address the limitations of existing upper limb robotic systems by providing active shoulder support through a mechanical structure intended for low-cost production. iPAM has a dual robotic design similar to the REHAROB system, but with a total of six active DOFs (see Fig. 1). Each robot is actuated using electropneumatic servovalves and low-friction pneumatic cylinders. This provides a clean, high power-to-weight power source resulting in an inherently compliant system that is suited to human interaction, even in a passive or unpowered state. Force transducers on each robot measure the robot–human interaction forces.

The configuration of the iPAM robots and patient is analogous to a therapist holding the patient's upper limb during conventional therapy. The resultant six controlled DOFs allow control strategies that support and assist coordinated movement of the upper limb as a whole, rather than just the movement of the forearm or hand. For further details on the mechanics and hardware of the iPAM system, see [12]. The iPAM system is currently undertaking the second of two exploratory clinical trials. A total

Manuscript received December 3, 2008; revised June 2, 2009; accepted August 3, 2009. Date of publication September 25, 2009; date of current version July 28, 2010. Recommended by Technical Editor G. Morel. This work was supported by the U.K. National Institute for Health Research.

P. R. Culmer, A. E. Jackson, R. Richardson, and M. C. Levesley are with the School of Mechanical Engineering, University of Leeds, Leeds, LS2 9JT, U.K. (e-mail: p.r.culmer@leeds.ac.uk; a.e.jackson@leeds.ac.uk; r.c.richardson@leeds.ac.uk; m.c.levesley@leeds.ac.uk).

S. Makower is with the Leeds Primary Care National Health Service Trust, Leeds, LS12 3QE, U.K. (e-mail: s.makower@leeds.ac.uk).

J. A. Cozens is with the Department of Rehabilitation Medicine, Grampian National Health Service, Aberdeen, AB25 2ZA, U.K. (e-mail: alastair.cozens@arh.grampian.scot.nhs.uk).

B. B. Bhakta is with the Faculty of Medicine and Health, University of Leeds, Leeds LS2 9JT, U.K., and also with Leeds Teaching Hospitals National Health Service Trust, Leeds LS9 7TF, U.K. (e-mail: b.bhakta@leeds.ac.uk).

Digital Object Identifier 10.1109/TMECH.2009.2030796

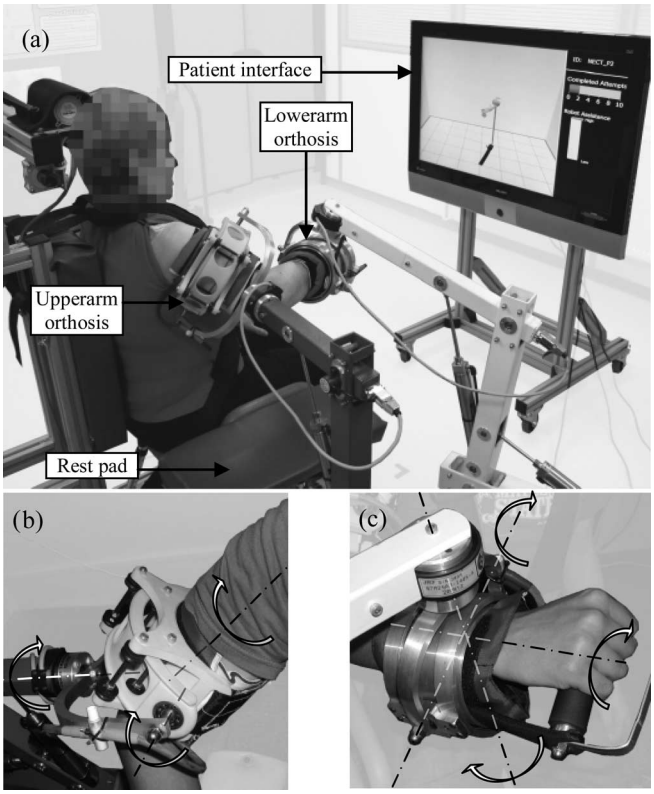

Fig. 1. (a) iPAM system assisting a patient through a therapeutic exercise. (b) Free DOFs on the upper orthosis. (c) Free DOFs on the forearm orthosis.

of 36 stroke patients have used the system, accumulating over 300 h of robot-mediated therapy.

The requirements and development of iPAM's assistive control scheme are discussed in Section II and implementation issues are detailed in Section III. Evaluation of the control scheme is presented in Section IV, followed by results, discussion, and conclusion in Sections V, VI, and VII.

II. Cooperative Control Scheme

A. Controller Aims and Objectives

Requirements for the iPAM controller fall into clinical and engineering categories.

1) Clinical Factors: Recovery of upper limb function after stroke depends on motor learning [13]. This study is built on well-established hypotheses for motor learning [14] that specifies a need for:

1) intensive, repeated practice of movements;
2) realistic task-based activities;
3) active participation of the subject in the task;
4) coordinated upper limb movement patterns.

Therapeutic movements should be properly supported to avoid secondary complications, for example, shoulder pain.

The iPAM project has had strong clinical input throughout; this is crucial for ensuring that the system addresses real issues and approaches them in a way that is practical for clinical adoption. Treatment will typically be offered to patients across a series of sessions. The system must store patient data (including prescribed exercise tasks) and reload these in subsequent sessions, thus encouraging repeated practice of particular movements.

2) Engineering Factors: The kinematic arrangement of the combined robot–patient system is central to the engineering demands. Each robot has three active DOFs, and assists the patient via two custom orthoses: the first located on the lower arm and the second on the upper arm. Each orthosis has an inflatable insert lined with high-friction material (Tensowrap) to ensure a comfortable, but snug fit. The robots control the Cartesian position of the center of each orthosis; the orthoses three rotational DOFs are unconstrained and intersect with the arm segment's longitudinal axis. The rotations are achieved in each orthosis using two pivots in combination with a circular slider acting about the arm segment's longitudinal axis, as shown in Fig. 1. This allows natural orientation of the upper limb and prevents undesirable torques from being exerted. The upper and lower orthoses are located by the elbow and wrist, respectively, to minimize the effect of soft-tissue deformations.

To safely coordinate movement of the patient's limb and avoid harmful force or motion, the control scheme must be cooperative to ensure that the robots act in unison with each other, and with the patient's arm.

3) Approach: The cooperative control scheme presented in this section is summarized in Fig. 2. The human upper limb is the common object of interest to both robots. Therefore, the movement of the compound robot–human system is expressed with respect to the upper limb, and then mapped to each individual robot. This is accomplished by developing a kinematic model of the upper limb with respect to the attachment points of each robot to define a global upper limb coordinate system. By abstracting the main coordinate system to the upper limb, the movement trajectories are independent of the system's physical configuration, especially the size and positioning of the robots and upper limb. This allows trajectories to be recorded once, and then used across different therapy sessions for individual patients. Forward and inverse kinematics for the upper limb model define the transformations between the upper limb coordinate system and each robot's Cartesian task space.

Impedance and admittance control provide an established mechanism to specify a dynamic relationship between position and force in a system, and provide controllable DOFs with definable degrees of compliance [15], [16]. This is well suited to human–robot interaction, and has been widely applied in rehabilitation robotics to vary the assistance provided by the robot, for example, see [6] and [16]–[18]. It is a common practice to use a mechanical analogue to define the relationship, for example, a mass–spring–damper arrangement

$$\text{Admittance: } P_d = P_t + \frac{F_i}{k + cs + ms^2}$$
$$\text{Impedance: } F_d = F_t + P_i\left(k + cs + ms^2\right) \quad (1)$$

where P and F denote position and force, subscript d is the controller demand, t is the original trajectory, i is the measured interface force or deflection, s is the Laplace differential, and m, k, and c are the mass, spring, and damping parameters. Inspecting (1) shows that the admittance form requires an inner

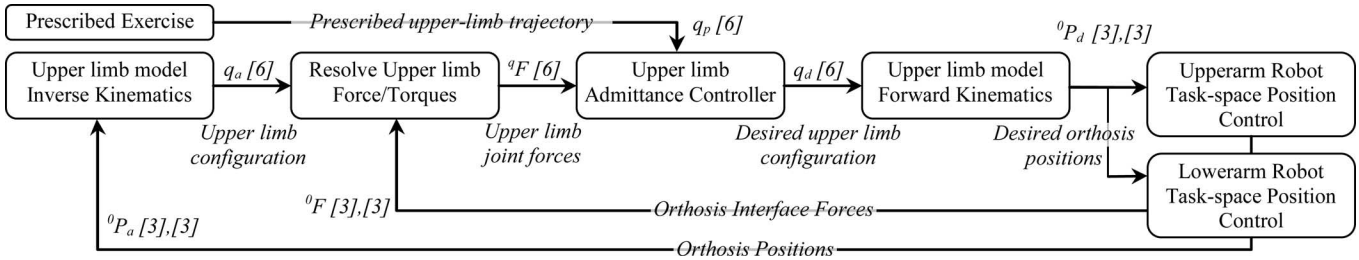

Fig. 2. Schematic of the iPAM upper limb cooperative control scheme.

position controller, while the impedance form requires a force controller. In both cases, the demand signal is derived by modulating the original trajectory according to the modeled dynamic relationship.

iPAM's pneumatic actuation intuitively suggests the use of an impedance control scheme because pressure control using servovalves is well established. However, previous work [19] has found that nonlinear effects inherent in pneumatics, for example, stiction, make accurate force control of a moving cylinder problematic, but they are less significant in position control. This favors an admittance rather than impedance control scheme for iPAM.

iPAM uses an admittance control scheme that operates in the upper limb coordinate system. The admittance controller uses upper limb joint forces/torques, which are resolved from robot–human interface forces using the upper limb model. This is consistent with expressing movement trajectories relative to the upper limb, and importantly, allows the system to direct assistance at moving specific joints of the upper limb in isolation. For example, during a reaching task, the clinical assessment may demand greater assistance for elbow extension than shoulder flexion; therefore, the controller would be set to provide high assistance for elbow extension, but low assistance for shoulder flexion. The level of assistance can, thus, be precisely tailored to individual patient needs.

B. Kinematic Upper Limb Model

1) Model Considerations: The kinematic model of the upper limb is merely intended to provide the foundation for the control scheme, rather than being comprehensively anatomical. A compromise between model accuracy and computational complexity is required for practical implementation, particularly with regard to the inverse kinematics solution.

A human limb has layers of skin, fat, connective tissue, muscle, and bone that move in relation to one another. The limb has complex joints whose axes of rotation can change during movement. These factors can lead to difficulties in modeling the system. Modeling the limb as a set of rigid bodies using the following assumptions provides a pragmatic solution to this complex problem [20].

1) The deformation of soft tissues does not significantly affect the mechanical properties of the limb segment as a whole.
2) Within each segment (forearm and upper arm), bones and connective tissues have similar rigid-body motions.

These assumptions allow the use of rigid-body kinematic modeling techniques that are widely used in robotics.

The shoulder is composed of movement of the glenohumeral and scapulathoracic joints, resulting in complex rotational and translational movements [21]. A 5-DOF model has been selected [22] that approximates the gross compound movements of the shoulder without requiring detailed modeling of the internal elements. A spherical joint models the glenohumeral joint. Two translational DOFs represent scapular movement relative to the thorax. Higher order models (for example, see, [23]) would introduce kinematic redundancies with respect to the 6-DOF robot system that could not be directly controlled. The upper arm is treated as a single link to the elbow joint. The elbow joint is then approximated to a single-DOF hinge joint, consistent with the literature [24]. Movement at the wrist and hand are not included in the model as they are not actively assisted by the robot system. Although the lower arm orthosis allows freedom of movement about the longitudinal axis of the forearm (pronation and supination), they are not actively controlled by the robot. The trunk will be assumed to be held stationary by a harness while the patient is using the iPAM system. In some patients, abnormal compensatory movements by the patient can occur while attempting to undertake voluntary reaching movements. The harness seeks to minimize these by constraining movement of the thorax.

2) Model Definition: The Denavit–Hartenburg framework [25] has been used to assign coordinate frames to the links of the upper limb model described in the previous section. Fig. 3 shows the chain of coordinate frames and orthosis positions of the robots. The fixed shoulder origin is defined by coordinate frame 0 (F_0) and represents the global Cartesian task space common to both robots. The upper limb coordinate system that provides the basis for the control scheme is expressed in terms of the variables $d_1, d_2, \theta_3, \theta_4, \theta_5$, and θ_6. The upper and lower orthoses are defined by F_{5b} and F_6.

3) Forward Kinematics: The forward kinematics of the upper limb model provides a mapping from upper limb joint coordinates to the position of the two orthoses in global Cartesian task space

$$\begin{bmatrix} {}^0P_{\text{upper}} \\ {}^0P_{\text{lower}} \end{bmatrix} = FK\,(q)$$

where

$$^0P = \left[{}^0x, {}^0y, {}^0z\right]^T \quad q = d_1, d_2, \theta_3, \theta_4, \theta_5, \theta_6. \qquad (2)$$

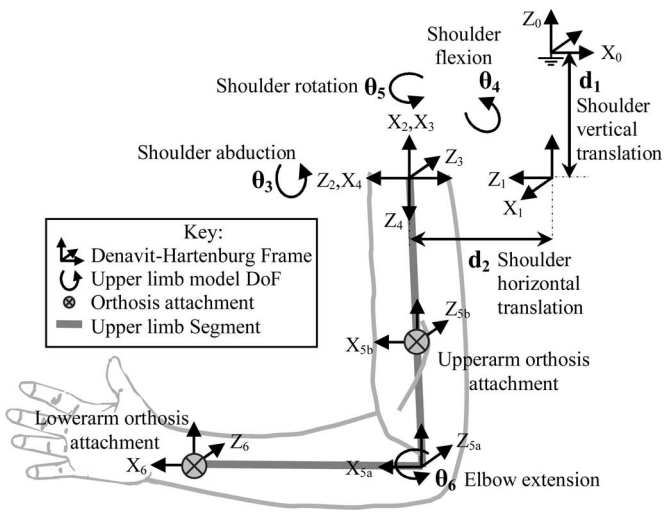

Fig. 3. 6-DOF upper limb model assigned with Denavit–Hartenburg coordinate frames. Clinical descriptors of each DOF are provided for convenience and defined with the arm in the anatomical position shown. Upper limb length parameters are defined with respect to the coordinate frames: $L_{\mathrm{u1}} = F_2 \rightarrow F_{5\mathrm{a}}$, $L_{\mathrm{u2}} = F_2 \rightarrow F_{5\mathrm{b}}$, and $L_l = F_{5\mathrm{a}} \rightarrow F_6$.

TABLE I
DENAVIT–HARTENBURG PARAMETERS FOR THE UPPER LIMB MODEL

Link	α_i	A_i	θ_i	D_i
1	$\pi/2$	*0*	$\pi/2$	d_1
2	0	*0*	$\pi/2$	d_2
3	$-\pi/2$	*0*	θ_3	0
4	$\pi/2$	*0*	$\theta_4 - \pi/2$	0
5a	$-\pi/2$	*0*	θ_5	L_{u1}
5b	$-\pi/2$	*0*	θ_5	L_{u2}
6	0	L_l	θ_6	0

This is derived by calculating the transformation between the global task space F_0, and the upper and lower orthoses $F_{5\mathrm{b}}$ and F_6, respectively. Transformations between successive coordinate frames are calculated using 4×4 transformation matrices derived from the model's Denavit–Hartenburg parameters, which are detailed in Table I. The resultant transformation for each orthosis is obtained from the product of the chain of transformations as

$$
\begin{aligned}
{}^0T_{\mathrm{upper}} &= {}^0T_1\,{}^1T_2\,{}^2T_3\,{}^3T_4\,{}^4T_{5\mathrm{b}} \\
{}^0T_{\mathrm{lower}} &= {}^0T_1\,{}^1T_2\,{}^2T_3\,{}^3T_4\,{}^4T_{5\mathrm{a}}\,{}^{5\mathrm{a}}T_6.
\end{aligned} \tag{3}
$$

The resultant 4×4 matrices in (3) specify both the orientation and position of the orthosis frames in global task space. Only positional information is required for the controller, since the orientation of the end- effectors is unconstrained. This is found directly from the position subset of the transformation matrices in (3). The forward kinematics are a function of the upper limb parameters L_{u1}, L_{u2}, and L_l. These parameters define the position of the orthoses on the upper limb and remain constant for a given treatment session. They may vary between sessions through slight differences in the placement of the orthoses on the upper limb and between people according to the size of the upper limb.

4) Inverse Kinematics: The inverse kinematics of the upper limb model define the mapping from the orthosis positions to the upper limb joint configuration and perform the inverse operation to (2).

Given the kinematic configuration of the upper limb model, it is possible to derive a unique closed-form solution from geometric analysis of Fig. 3. However, tests of the practical implementation revealed that it has poor robustness to measurement error, particularly in upper limb configurations that approach kinematic singularities.

An alternative numerical estimation technique has been implemented using the Jacobian transpose inverse kinematics technique [26]. This iterative method uses the differential properties of the Jacobian matrix to minimize error, and hence, estimates a solution to the inverse kinematics, and is summarized by the difference equation

$$
q_t = q_{t-1} + \left(\begin{bmatrix} {}^0P_{\mathrm{upper}} \\ {}^0P_{\mathrm{lower}} \end{bmatrix} - FK\left(q_{t-1}\right) \right) J^T\left(q_{t-1}\right) K \tag{4}
$$

where K is a gain that determines the rate at which the method converges toward the inverse kinematics solution and must be bounded to prevent an oscillatory response.

This method has two valuable properties: 1) it only requires computation of the direct forward kinematics, which is straightforward [27] and 2) it is numerically stable at kinematic singularities [25], unlike the direct closed-form inverse kinematics. Testing revealed the Jacobian transpose method to be accurate and robust to the disturbances found during routine use of the iPAM system [12].

C. Upper Limb Admittance Controller

The admittance controller can define any dynamic relationship between position and force. In this case, a spring–damper arrangement is appropriate; the stiffness term defines the low-frequency compliance of the system, whilst the damping term is used to prevent undesirable oscillations. A spring–damper form of admittance controller about the upper limb coordinate system is defined as

$$
q_d = q_p + \frac{{}^qF}{k + cs} \tag{5}
$$

where ${}^qF$ are the interface forces/torques, k and c are the stiffness and damping parameters, q_p is the original prescribed movement, and q_d is the position demand. All variables are with respect to the upper limb coordinate system, and are shown in Fig. 2. Inspecting (5) shows it has the desired properties; when k is high, $q_d \rightarrow q_p$ and the admittance controller acts like a position controller, effectively providing high assistance. Accordingly, the maximum assistance that can be achieved is defined by the performance of the underlying position controller. As k is lowered, q_d deviates from q_p as a function of the measured interaction force, and hence, provides less assistance.

To implement the admittance controller in (5) requires a measurement of ${}^qF$. This must be derived by transforming the interface forces measured at the two robot orthoses into the upper

limb coordinate system. A Jacobian transpose matrix of the upper limb model is used to achieve this transformation. This method employs the principle of virtual work: The work done by a force/torque in joint space is equal to the work done by a force/torque in the Cartesian task space [27] as

$$^{q}F = J^{T}(q)\,^{0}F \tag{6}$$

where

$$^{q}F = [f_{d1}, f_{d2}, \tau_3, \tau_4, \tau_5, \tau_6] \quad ^{0}F = [f_{x1}, f_{y1}, f_{z1}, f_{x2}, f_{y2}, f_{z2}].$$

III. Controller Implementation

The upper limb cooperative control scheme is used on the iPAM system. A number of practical factors have been addressed to ensure that it is appropriate for routine clinical use.

A. Real-Time Architecture

The entire iPAM control scheme (see Fig. 2) is a time-critical process operating at 500 Hz, which demands deterministic reliable operation. To meet these demands, it is implemented on a real-time platform (National Instruments LabVIEW Real-time v8.2) on a dedicated PC.

A therapist interface has been developed to facilitate routine clinical use of the system. It provides the ability to store and retrieve patient records (e.g., movement trajectories, assistance settings, and performance measures), define new movement trajectories, and prescribe iPAM therapy programs by appropriately instructing the real-time controller PC. The user interface (UI) is implemented on a separate PC that communicates with the real-time PC via a TCP/IP network link. Communication processes are asynchronous to prevent disruption of the time-critical control loop.

B. Low-Level Position Control

Referring to Fig. 2, the low-level position controller tracks the position demand in task space "$^{\circ}P_d$" for each robot. The control scheme used by each of the iPAM robots is based on the PID control scheme with feedforward force compensation described in [16]. Additional terms compensate for the weight of the robot links and orthoses. This allows iPAM to appear weightless to the user and therapist, thus helping to reduce fatigue and the risk of joint strain.

The key requirements for the position control scheme are stable operation and accurate position tracking. The human context of this study demands that safe operation is given precedence. Therefore, the controller was tuned conservatively to ensure a large stability margin at the expense of some position tracking performance. Physical testing found a suitable configuration, which resulted in the performance presented in Table II.

C. Safety Considerations

User safety must be a priority with robots that interact with humans, and particularly, in this case because people with stroke are often more susceptible to injury. A number of safeguards have been implemented to protect the user, which are as follows.

TABLE II
Task-Space Position-Tracking Performance of a Single iPAM Robot

	X	Y	Z
Error RMS (mm)	23.6	16.9	11.3
Error STD (mm)	0.15	0.36	0.31

Data collected using a single iPAM robot to move a passive mechanical human arm model [11] through a reach–retrieve movement via a forearm attachment. The arm was configured to represent a 50th percentile male. The rms and standard deviation (STD) are reported for five repetitions of the movement. Each repetition lasted 30 s.

TABLE III
iPAM Robot Components

Component	Model	Details
Pneumatic actuators	Airpot *M24 D15 U*	Stroke: 150mm Max. pressure: 0.7 MPa
Electro-pneumatic servo valves	Norgren *VP51*	Max. output pressure: 1 MPa Control signal: 0-10V
6 DOF force transducers	JR3 *67M25*	Max. force X,Y: 222N, Z: 444N Max. torque: ± 14.9 Nm

1) *Controller watchdog:* A watchdog module monitors controller signals to prevent excessive force or fast motion being exerted on the upper limb (e.g., as a result of component failure). Erroneous events result in a "soft" controlled shutdown for noncritical errors and a "hard" immediate shutdown for critical events.
2) *Bounded upper limb configuration demand:* To prevent an abnormal or uncomfortable upper limb configuration, the admittance controller output is bounded to safe limits. For example, the elbow joint is limited to 180° extension. This is secondary to the expertise of the operating therapist who ensures that the desired movement is safe and appropriate for a given individual.
3) *User and emergency stops:* An easily accessible user-stop switch smoothly returns the upper limb to a predefined comfortable position, typically resting on a support pad to their side. This allows the user or therapist to stop the system in the event of fatigue or discomfort. An emergency stop cuts all power to the system to make iPAM completely passive.

D. Equipment

iPAM was developed specifically for assisting upper limb movements. The development process of the robots, orthoses, and optimization of the upper limb workspace are discussed in [9]. The components central to the control scheme are presented in Table III. The pneumatic actuators have low-friction characteristics that make them ideal for control applications. The servovalves are high-speed pressure-control models with customizable gain settings that allow tuning for optimum performance with the position controller.

IV. Controller Testing

The iPAM system was comprehensively tested before clinical trials to ensure satisfactory controller robustness and performance in real-world conditions. Testing was undertaken in two main stages: first, computational simulations were used to

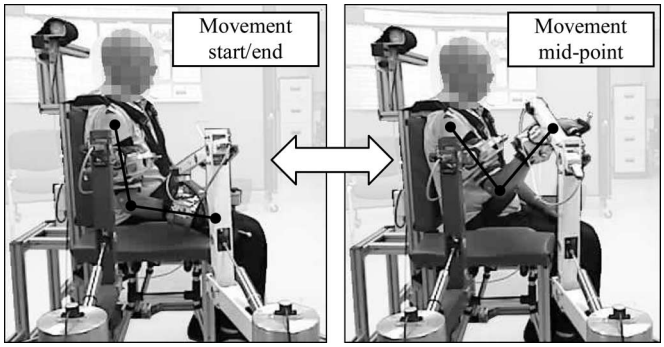

Fig. 4. Hand-to-mouth testing movement seen in the sagittal plane.

verify the idealized behavior of the system, and second, physical testing was conducted on the iPAM system. Physical testing was initially conducted using a passive mechanical upper limb model before progressing to healthy subjects, and finally, into exploratory clinical trials with stroke patients.

A. Experimental Setup

In this paper, the properties and performance of the cooperative admittance control scheme are illustrated by comparing data from a single-stroke patient undertaking iPAM-assisted movement with an idealized simulation test case of the same movement. The simulation gives a generalized case from which common trends can be identified, rather than directly approximating the patient's limb anatomy (e.g., segment lengths, masses, or joint tone), which would be difficult to ascertain and validate. In both cases, the upper limb is *passive*; this illustrates the controller's capabilities without active patient input that would be difficult to quantify.

1) Movement Trajectory: The movement trajectory was prescribed by a therapist specifically for the stroke subject discussed in this paper. The therapist assisted the stroke subject through the movement with the iPAM system attached and passive. iPAM recorded the kinematics of this movement in terms of human upper limb coordinates ("q_p" in Fig. 2). This is typical of the procedure used to define therapeutic movements for the iPAM system. The same recorded trajectory could be applied to the simulation because the upper limb coordinates are independent of the upper limb lengths.

Fig. 4 depicts the recorded movement as assisted by iPAM, showing the start/end and midpoint of the trajectory. It equates to a hand-to-mouth movement, where the predominant components are a combination of shoulder and elbow flexion. It is, consequently, an ideal movement for illustrating the ability of the controller to assist coordinated movement.

2) Controller Configurations: iPAM can be set to provide any number of different controller assistance permutations for a particular movement. Three test cases will be used to illustrate the effects of altering controller assistance about specific upper limb DOFs in isolation and combination through the hand-to-mouth movement. The test cases, defined in Table IV, cover a combination of assistance levels for shoulder and elbow flexion, which are the main DOFs involved in the movement.

TABLE IV
UPPER LIMB CONTROLLER ASSISTANCE CONFIGURATIONS

Test case	Shoulder Flexion (θ_4)	Elbow Flexion (θ_6)	Remaining DOFs
1	High: A=1	High: A=1	High: A=1
2	Low: A=0.1	High: A=1	High: A=1
3	High: A=1	Low: A=0.1	High: A=1

The assistance value (A) is converted to values of c and k by:
d_1 and d_2: $c = 80\ \mathrm{N{\cdot}s^{-1}m^{-1}}$; θ_1–θ_6: $c = 0.25\ \mathrm{N{\cdot}m{\cdot}s^{-1}deg^{-1}}$.
d_1 and d_2: $k = 10\,000\mathrm{A\ N{\cdot}m^{-1}}$; θ_1–θ_6: $k = 3\mathrm{A\ N{\cdot}m{\cdot}deg^{-1}}$.

TABLE V
UPPER LIMB PROPERTIES FOR THE SIMULATION TEST CASE

Property	Upperarm		Lowerarm	Hand
Segment length (m)	0.304		0.275	0.191
Segment CoM* (m)	0.132		0.117	0.07
Segment mass (Kg)	2.1		1.2	0.4
	d_1	d_2	θ_3, θ_4, θ_5	θ_6
Damping ($\mathrm{N{\cdot}s^{-1}m^{-1}}$, $\mathrm{N{\cdot}m{\cdot}s^{-1}deg^{-1}}$)	2.3×10^{-3}	1.8×10^{-3}	0.021	0.004
Stiffness ($\mathrm{N{\cdot}m^{-1}}$, $\mathrm{N{\cdot}m{\cdot}deg^{-1}}$)	5.1×10^{-3}	3.3×10^{-3}	0.524	0.019

*Centre of Mass (CoM) is defined from proximal end. Data from [27] and [28].

The high assistance level is the maximum that the iPAM system can provide; it aims to move a passive upper limb through the original movement defined by the therapist. Referring to (5), this requires a high stiffness (k) in the admittance controller. The low assistance level is defined with k at 10% of the high value. The damping level (c) is at a constant level, which is sufficient to prevent oscillatory response without inhibiting free movement.

3) Simulation Test Case: A simplified simulation of the iPAM system was developed to evaluate the idealized behavior of the cooperative control scheme. The simulation consists of a rigid-body upper limb model and the upper limb admittance controller acting about the model DOFs. For clarity, the low-level position control of the individual robots is assumed ideal, and is therefore neglected. An inverse dynamics solver determined the necessary assistive upper limb joint torques for the movement (Mathworks SimMechanics).

The upper limb model shares the 6-DOF kinematic arrangement shown in Fig. 3, and is configured using anthropometric data for a 50th percentile male. This forms a useful generalized test case for the control scheme with regard to expected joint forces/torques and displacements. Segment length and mass properties for the model are presented in Table V. Inertial properties are taken from the literature [28].

Passive joint properties are assigned to each upper limb DOF to account for physiological factors, for example, damping from soft tissues, and stiffness from muscle, tendon, and ligament groups. The compound effects of these passive mechanisms are approximated in each DOF by a second-order spring–damper system. Parameters for the translational shoulder DOFs d_1 and d_2 were obtained by averaging data for each plane from [30]. The rotational shoulder DOFs (θ_3, θ_4, and θ_5) were configured with data from [31] determined for passive shoulder abduction/adduction. Data were readily available for the elbow DOF (θ_6) [24].

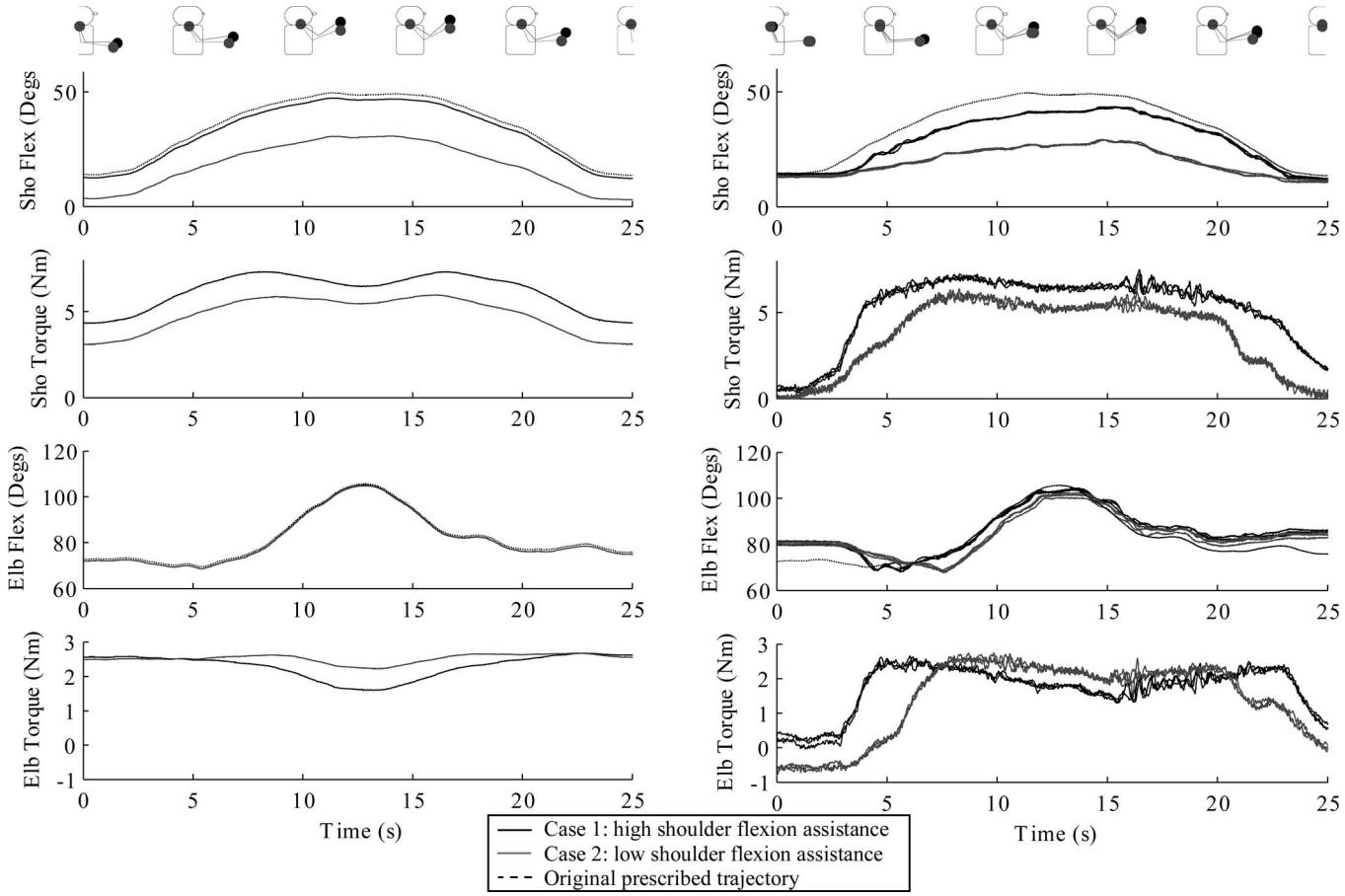

Fig. 5. Comparison of (left) simulated and (right) patient movements, and assistive torques for two levels of shoulder flexion assistance. Pictorial representation is in the sagittal plane. Patient case shows all three repetitions.

4) Stroke Subject Test Case: The iPAM system is currently being used in an exploratory clinical trial to provide assisted therapeutic exercise using the full cooperative control scheme presented in this paper. It has been approved by the U.K. Medicines and Healthcare products Regulatory Agency (MHRA) for clinical investigation. The iPAM clinical trials have been approved by the Leeds Teaching Hospitals National Health Service (NHS) Trust Ethics Committee. Each subject has given written informed consent to take part in the studies.

The patient reported here is a 67-year-old male, three years poststroke. He has right-sided hemiplegia with minimal ability to make active contributions to forward reach movements, thus helping to ensure that the upper limb was passive during testing. Resistance to passive movement is low in the shoulder and elbow joints, and he was assessed by a research therapist to have a Fugl–Meyer score of 9/60.

A research therapist operates the system. Beginning a therapy session, the system is calibrated to determine the upper limb segment lengths and the orthosis positions relative to each segment. These are expressed as the parameters $L_{\mathrm{u}1}, L_{\mathrm{u}2}$, and L_l shown in Fig. 3, and determined by direct measurement using anatomical landmarks. The calibration parameters are necessary for the forward and inverse transformations between human joint coordinates and root task space described by (2) and (4), respectively. Thus, the same movement can be prescribed for arms of different sizes using the upper limb coordinate system and transformed to the necessary orthosis positions in robot task space using the appropriate calibration parameters.

The assistance configurations were defined for the movement trajectory using the iPAM therapist interface. iPAM was set to assist the subject through the three configurations sequentially, with three repetitions of each to allow for variation in response. The subject was asked to relax and remain passive throughout the movements. The visual display used to instruct and guide subjects through exercises was disabled to discourage active participation.

V. Results

All assistance configurations were conducted successfully with iPAM and the patient. No adverse events or discomfort during the movements were reported.

Referring to Table III, Fig. 5 compares cases 1 and 2 for the simulation and iPAM assisting the patient. The simulation highlights the general behavior of the cooperative controller. To achieve this movement with a passive upper limb, the system must provide the necessary motive force/torques about each DOF. These comprise dynamic components (such as joint

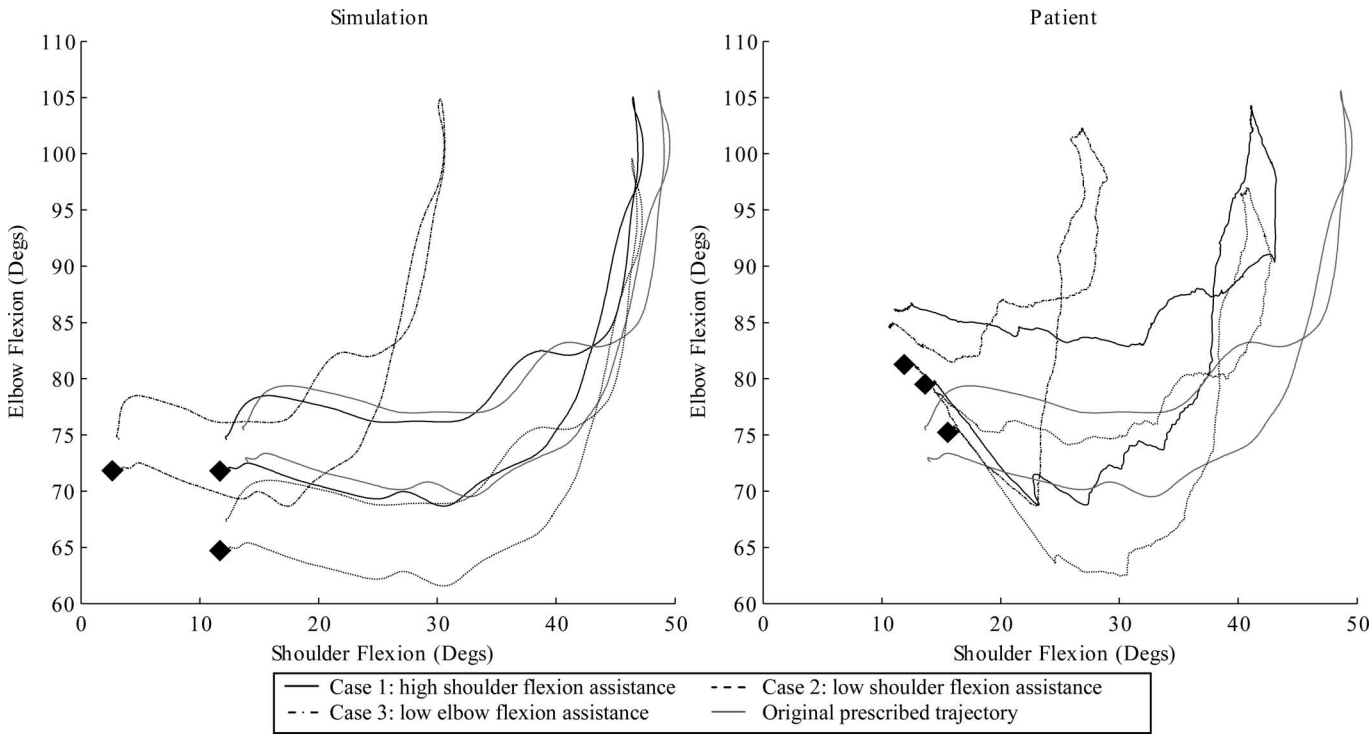

Fig. 6. Cyclograms of the assistance cases detailed in Table III. Patient case shows mean of all three repetitions. ♦ indicates movement start.

damping properties and segment inertias) and static components (including joint stiffness properties and forces/torques induced due to gravity). Decomposition in the simulation revealed that the gravitational components dominate in the torque responses.

In case 1, the upper limb achieves a high degree of shoulder flexion. As shoulder flexion increases, the torque about that DOF also increases to oppose the induced gravitational moment on the limb. The inflection in torque at the midpoint of the movement corresponds to the elbow flexing, reducing the gravitational lever arm of the combined upper limb, and hence, requiring less torque at the shoulder flexion DOF. Elbow flexion is concentrated toward the midpoint of the movement, as reflected in the elbow torque profile.

In case 2, the assistance about the shoulder flexion DOF is reduced. This results in lower flexion throughout the movement because the controller modulates the original trajectory as a function of the torque. However, the shoulder flexion movement and torque profiles have the same characteristics as case 1, so the pattern of movement is preserved. The elbow flexion in case 2 follows the same profile as in case 1, showing that the reduction in shoulder flexion assistance is particular to that DOF, while other DOFs remain independent; this confirms a key property of the cooperative control scheme The torque profile differs because the reduced shoulder flexion induces lower gravitational torques in the elbow.

The subject responses in Fig. 5 have high interattempt repeatability. This indicates that the iPAM system is consistent, and the subject remained passive—active involvement would be seen as disturbances in the torque profiles. The start and end sections of the movement show some discrepancies to the simulation; the torques are reduced and the movement in case 2 converges toward case 1. This can be attributed to physical contact between the subject's forearm and a rest pad (seen in Figs. 1 and 4) used to support the upper limb between movements. The support provided by the rest pad reduces the assistive force that iPAM needs to provide to attain the upper limb configuration, and consequently, the torques at the shoulder and elbow are reduced. Excepting the immediate start and end sections, the same characteristics described for the simulation can be seen in the movement and torque profiles for the subject; lower assistance in shoulder flexion results in reduced flexion, while the elbow profile retains the same profile as for full assistance. This demonstrates that the cooperative controller is effective in isolating and applying assistance to individual DOFs via the iPAM system.

With full assistance, there is reduction in the peak shoulder and elbow flexion achieved with the subject, compared to the simulation and original prescribed movement. The response of the admittance controller is bounded by the performance of the underlying position controller. The simulation assumes ideal position control (e.g., response exactly meets demand), which is impractical; therefore, some variation between the responses is inevitable.

The remaining test cases are consistent with the controller behavior illustrated in Fig. 5, with the same common trends between the simulation and subject test cases. In Fig. 6, the test cases are summarized in "cyclograms" that characterize the coordination between shoulder and elbow extension in the movement. The cyclogram for the full assistance case acts as a baseline and shows that the initial period of movement occurs mainly in shoulder flexion with the bias shifting toward elbow flexion at the midpoint of the movement, returning to shoulder flexion toward the end of the movement.

Case 2 in Fig. 6 illustrates a reduction in shoulder flexion assistance. The cyclogram is shifted to the left and compressed horizontally. This demonstrates a static reduction in shoulder flexion and a reduced range of movement. Elbow flexion is unaffected, so there is no shift or compression in this axis. Reducing the elbow assistance, as shown in case 3, produces a similar characteristic; the cyclogram is shifted downward and compressed. Both factors are less significant than for shoulder flexion because the torques about the elbow are lower, resulting in less modulation of the input trajectory by the admittance controller. The effects of altering the elbow assistance are isolated to this DOF; the shoulder flexion cyclogram is unaffected.

Note that the coordination pattern of the movement is preserved with respect to the high assistance case, despite reducing assistance levels in one or more joints. This derives from the coordination of the original movement being defined implicitly by the time-based trajectory of each joint DOF.

The cyclograms for the patient in Fig. 6 exhibit the same trends between the full and reduced assistance cases demonstrating that the cooperative controller is effective in a practical implementation. The simulation and subject cyclograms have similar profiles. Discrepancies are primarily due to the effects of the upper limb rest pad and practical limitations of the iPAM position control scheme compared to the idealized simulation. The joint properties of the subject may also deviate from the idealized spring–damper assumed in the simulation, and include time-variant artifacts that are difficult to quantify.

VI. Discussion

Patient data confirm that the control scheme exhibits the desired properties of variable assistance demonstrated in the simulation. This is crucial in encouraging the patient to engage in active exercise, and thus, promote motor learning—a key requirement in this paper.

While the simulation considers an idealized case, there are a number of significant issues inherent in the practical implementation of iPAM. The behavior of the upper limb admittance controller is dependent on the performance of the underlying position controller. This is principally affected by the pneumatic actuation used by iPAM with factors such as air compressibility and actuator stiction. In addition, it is essential to ensure that the system remains stable, and consequently, some tracking performance must be sacrificed to ensure a suitable stability margin. Position tracking errors are manifested in the upper limb admittance controller by cross-coupling between DOFs (e.g., altering the assistance about the elbow also has some effect at the shoulder), and the range of stiffness and damping characteristics that can be achieved. This is apparent to some degree in the patient results shown in Fig. 6. Thus, while the position controller provides satisfactory performance, there are opportunities for improvement in tracking and disturbance rejection. This is an area of ongoing work, and will take advantage of recent developments in pneumatic components and alternative control strategies.

Measurement error is minimized wherever possible in the iPAM system, but will always be significant in a robot–human application. A key factor is the deformation of soft tissues that result in the orthoses moving, albeit minimally, relative to the upper limb segments, consequently, inducing errors in the parameters L_{u2} and L_l. A major implication is the need for inverse kinematics that are robust to measurement error, as described previously. Additionally, it effects calculation of the upper limb joint configuration causing cross-coupling between the upper limb DOFs. This could potentially result in undesirable interaction between the two robot arms. However, during extensive use of iPAM, this has not been a significant factor. A key reason is the damping properties inherent in the admittance controller and the inflatable inserts of the orthoses that act to attenuate higher frequency vibration that may otherwise cause instability.

The therapist operating iPAM provides expert input by defining appropriate movements and levels of assistance for each patient. Manipulating the patient's arm in iPAM requires some readjustment from standard practice for the therapist, but it was found that smooth, therapeutically appropriate movements could be defined after a short learning curve. Translational movement at the shoulder was generally low (around ± 20 mm in each axis), which might suggest that these DOFs could be neglected. However, movements such as "hand-to-mouth" maneuvers result in larger displacements because of scapula rotation. iPAM aims to encompass these cases in order to offer a wide variety of functional exercises to patients. Consequently, the translational shoulder DOFs are deemed an important part of the system so that the shoulder is appropriately and actively supported.

VII. Conclusion

A cooperative control scheme has been developed that enables iPAM to deliver upper limb exercise therapy for stroke patients by coordinating movement of two robots relative to a kinematic model. It is clinically appropriate, and allows variable levels of assistance to be specified for each joint of the upper limb. The system was tested in simulation and with a patient without adverse events. In practice, the performance of the control system is affected by actuator properties and human factors. However, it was shown to be stable and effective at delivering variable assisted exercise during therapeutically appropriate movements.

Acknowledgment

The authors would like to thank the stroke subjects from their clinical trials and the Yorkshire Rehabilitation Technologies User Group who have given their time and effort to the project.

References

[1] U.K. Department of Health, "Reducing brain damage: Faster access to better stroke care," U.K. Department of Health, London, U.K., Rep. HC 452, 2005/2006.

[2] E. S. Lawrence, C. Coshall, R. Dundas, J. Stewart, A. G. Rudd, R. Howard, and C. D. Wolfe, "Estimates of the prevalence of acute stroke impairments and disability in a multiethnic population," *Stroke*, vol. 32, no. 6, pp. 1279–1284, Jun. 2001.

[3] R. W. Teasell and L. Kalra, "What's new in stroke rehabilitation: Back to basics," *Stroke*, vol. 36, no. 2, pp. 215–217, Feb. 2005.

[4] G. Kwakkel, B. J. Kollen, and H. I. Krebs, "Effects of robot-assisted therapy on upper limb recovery after stroke: A systematic review," *Neurorehabil. Neural Repair*, vol. 22, no. 2, pp. 111–121, 2008.
[5] H. Krebs, J. J. Palazzolo, L. Dipietro, M. Ferraro, J. Krol, K. Rannekleiv, B. T. Volpe, and N. Hogan, "Rehabilitation robotics: Performance-based progressive robot-assisted therapy," *Auton. Robots*, vol. 15, no. 1, pp. 7–20, Jul. 2003.
[6] R. Loureiro, "Upper limb robot mediated stroke therapy-gentle/s approach," *Auton. Robots*, vol. 15, no. 1, pp. 35–51, Jul. 2003.
[7] T. Nef, M. Mihelj, and R. Riener, "Armin: A robot for patient-cooperative arm therapy," *Med. Biol. Eng. Comput.*, vol. 45, no. 9, pp. 887–900, Sep. 2007.
[8] A. Gupta and M. K. O'Malley, "Design of a haptic arm exoskeleton for training and rehabilitation," *IEEE/ASME Trans. Mechatronics*, vol. 11, no. 3, pp. 280–289, Jun. 2006.
[9] J. C. Perry, J. Rosen, and S. Burns, "Upper-limb powered exoskeleton design," *IEEE/ASME Trans. Mechatronics*, vol. 12, no. 4, pp. 408–417, Aug. 2007.
[10] G. Fazekas, M. Horvath, and A. Toth, "A novel robot training system designed to supplement upper limb physiotherapy of patients with spastic hemiparesis," *Int. J. Rehabil. Res.*, vol. 29, no. 3, pp. 251–254, Sep. 2006.
[11] R. Riener, T. Nef, and G. Colombo, "Robot-aided neurorehabilitation of the upper extremities," *Med. Biol. Eng. Comput.*, vol. 43, no. 1, pp. 2–10, Jan. 2005.
[12] A. E. Jackson, R. J. Holt, P. R. Culmer, S. G. Makower, M. C. Levesley, R. C. Richardson, J. A. Cozens, M. Mon-Williams, and B. B. Bhakta, "Dual robot system for upper limb rehabilitation after stroke: The design process," *Proc. Inst. Mech. Eng. C, J. Mech. Eng. Sci.*, vol. 221, no. 7, pp. 845–857, 2007.
[13] R. J. Nudo, "Adaptive plasticity in motor cortex: Implications for rehabilitation after brain injury," *J. Rehabil. Med.*, vol. 35, no. 41, pp. 7–10, May 2003.
[14] N. Byl, J. Roderick, O. Mohamed, M. Hanny, J. Kotler, A. Smith, M. Tang, and G. Abrams, "Effectiveness of sensory and motor rehabilitation of the upper limb following the principles of neuroplasticity: Patients stable poststroke," *Neurorehabil. Neural Repair*, vol. 17, no. 3, pp. 176–191, 2003.
[15] N. Hogan, "Impedance control: An approach to manipulation: I—Theory. II—Implementation. III—Applications," *J. Dyn. Syst., Meas., Control*, vol. 107, no. 1, pp. 1–24, 1985.
[16] R. Richardson, A. Jackson, P. Culmer, B. Bhakta, and M. C. Levesley, "Pneumatic impedance control of a 3-d.o.f. physiotherapy," *Adv. Robot.*, vol. 20, no. 12, pp. 1321–1339, 2006.
[17] R. Colombo, F. Pisano, S. Micera, A. Mazzone, C. Delconte, M. C. Carrozza, P. Dario, and G. Minuco, "Robotic techniques for upper limb evaluation and rehabilitation of stroke patients," *IEEE Trans. Neural Syst. Rehabil. Eng.*, vol. 13, no. 3, pp. 311–324, Sep. 2005.
[18] L. Masia, H. I. Krebs, P. Cappa, and N. Hogan, "Design and characterization of hand module for whole-arm rehabilitation following stroke," *IEEE/ASME Trans. Mechatronics*, vol. 12, no. 4, pp. 399–407, Aug. 2007.
[19] R. Richardson, M. Brown, B. Bhakta, and M. C. Levesley, "Design and control of a three degree of freedom pneumatic physiotherapy robot," *Robotica*, vol. 21, no. 6, pp. 589–604, 2003.
[20] W. Maurel and D. Thalmann, "A case study on human upper limb modelling for dynamic simulation," *Comput. Methods Biomech. Biomed. Eng.*, vol. 2, no. 1, pp. 65–82, 1999.
[21] D. A. Neumann, *Kinesiology of the Musculoskeletal System*, 1st ed. St. Louis, MO: Mosby, Mar. 2002.
[22] M. A. Buckley and G. R. Johnson, "Computer simulation of the dynamics of a human arm and orthosis linkage mechanism," *Proc. Inst. Mech. Eng. H, J. Eng. Med.*, vol. 211, no. 5, pp. 349–357, Nov. 1997.
[23] F. C. Van Der Helm, "Analysis of the kinematic and dynamic behavior of the shoulder mechanism," *J. Biomech.*, vol. 27, no. 5, pp. 527–550, 1994.
[24] P. H. Mccrea, J. J. Eng, and A. J. Hodgson, "Linear spring–damper model of the hypertonic elbow: Reliability and validity," *J. Neurosci. Methods*, vol. 128, no. 1/2, pp. 121–128, Sep. 2003.
[25] B. Siciliano, "Kinematic control of redundant robot manipulators: A tutorial," *J. Intell. Robot. Syst.*, vol. 3, no. 3, pp. 201–212, 1990.
[26] L. Sciavicco and B. Siciliano, *Modelling and Control of Robot Manipulators*. New York: Springer-Verlag, Jan. 2000.
[27] C. Canudas, B. Siciliano, and G. Bastin, *Theory of Robot Control*, 1st ed. New York: Springer-Verlag, 1996.
[28] W. T. Dempster, "Space requirements of the seated operator," Wright-Patterson Air Force Base, OH, WADC Tech. Rep. TR-55-159 (1955), 1955.
[29] D. B. Chaffin, G. B. J. Andersson, and B. J. Martin, *Occupational Biomechanics*, 3rd ed. New York: Wiley, 1999.
[30] M. Makhsous, F. Lin, and L.-Q. Zhang, "Multi-axis passive and active stiffnesses of the glenohumeral joint," *Clin. Biomech.*, vol. 19, no. 2, pp. 107–115, Feb. 2004.
[31] L. Q. Zhang, G. H. Portland, G. Wang, C. A. DiRaimondo, G. W. Nuber, M. K. Bowen, and R. W. Hendrix, "Stiffness, viscosity, and upper-limb inertia about the glenohumeral abduction axis," *J. Orthop. Res.*, vol. 18, no. 1, pp. 94–100, Jan. 2000.

Peter R. Culmer received the M.Eng. degree (first class) in mechatronics and the Ph.D. degree in the control of a robotic system for arm rehabilitation from the School of Mechanical Engineering, University of Leeds, Leeds, U.K., in 2001 and 2007, respectively.

He is currently a Research Fellow in the School of Mechanical Engineering, University of Leeds. He is also working with a multidisciplinary team, and has experience in clinical evaluation of technology in adults and children. He specializes in applying computational modeling, control, and measurement techniques to human interface applications. He is also actively involved in enhancing learning and teaching through the adoption of new Web technologies. His current research interests include developing technology to improve function and quality of life in people with disability.

Andrew E. Jackson received the B.Eng. degree in mechatronics and the Ph.D. degree in vehicle dynamics and control from the University of Leeds, Leeds, U.K., in 1999 and 2004, respectively.

He was engaged in individual wheel control of a 6×6 hybrid electric off-road vehicle incorporating traction control, antilock braking, and direct yaw-moment control. He is currently a Research Fellow in the School of Mechanical Engineering, University of Leeds. His current research interests include rehabilitation robotics. He is involved in the iPAM project—a robotic rehabilitation system for the upper limb which has received two National Health Service Prizes for innovation.

Sophie Makower received the B.A. (Hons.) degree (Collegiate) from the University of Leeds, Leeds, U.K., in 1985, and the Graduate Diploma in physiotherapy from St. Thomas's Hospital, London, U.K., in 1989.

She has worked with stroke patients in a variety of settings and has completed postgraduate specialist neurology training courses. She is currently a Research Physiotherapist in the Leeds Primary Care National Health Service Trust, Leeds, and is engaged in the Intelligent Pneumatic Arm Movement Project.

Robert Richardson received the B.Eng. degree in mechatronics and the Ph.D. degree from the University of Leeds, Leeds, U.K., in 1997 and 2001, respectively.

During January 2001, he was a Postdoctoral Research Fellow at the University of Leeds, where he was a Teaching Fellow during January 2002, and has been a Lecturer of engineering systems and design in the School of Mechanical Engineering since 2008. He was engaged in the design, control, and actuation of a cardiac assist device. During April 2003, he was a Lecturer in robotics in the Department of Computer Science, University of Manchester, U.K., as part of the Artificial Intelligence Group, where he was also responsible for undergraduate and M.Sc. courses in robotics. His current research interests include rehabilitation robotics, robot and human interaction, modern actuator systems, and advanced control systems.

Dr. Richardson is a Chartered Member of the Institution of Mechanical Engineers.

J. Alastair Cozens received the B.Med.Sci., M.B.B.S., and M.D. degrees from Newcastle University, Newcastle upon Tyne, U.K., and the FRCS from Edinburgh.

He is a Consultant in rehabilitation medicine in the Department of Rehabilitation Medicine, Grampian National Health Service, Aberdeen, U.K., and specializes in the posture and movement rehabilitation of people with neurological disability. His current research interests include mechanisms of motor learning after stroke and the development of clinically based control systems for therapeutic devices.

Martin C. Levesley received the Ph.D. degree from the Department of Mechanical Engineering, Southampton University, Southampton, U.K.

He was a Postdoctoral Researcher at Southampton University, where he was engaged in research on aeroengine vibration control, in collaboration with Rolls Royce. In 1997, he joined the School of Mechanical Engineering, University of Leeds, Leeds, U.K., where he was the Director of the Institute of Engineering Systems and Design during 2006, and is currently the Director of Learning and Teaching. His current research interests include research on next-generation healthcare devices.

Dr. Levesley was the Chair of Dynamics and Control in 2008. He received a prestigious National Teaching Fellowship Award in 2009.

Bipin B. Bhakta received the B.Sc. (Hons.) degree in medical biochemistry, the M.B.Ch.B. and M.D. degrees from the University of Manchester, Manchester, U.K., and the MRCP and FRCP from Royal College of Physicians, London, U.K.

He is the Head of the Faculty of Medicine and Health, Academic Department of Rehabilitation Medicine, University of Leeds, Leeds, U.K. He is also a National Health Service (NHS) Consultant Physician in rehabilitation medicine at the Leeds Teaching Hospitals NHS Trust, Leeds. His research interests include development of restorative rehabilitation technologies, clinical trials, qualitative research, health outcome and educational assessment, and vocational rehabilitation research.